Proc. Natl. Acad. Sci. USA
Vol. 82, pp. 713–716, February 1985
Biochemistry

Active site structures of deoxyhemerythrin and oxyhemerythrin

(difference electron densities/crystallography/oxygenation mechanism)

RONALD E. STENKAMP*, LARRY C. SIEKER*, L. H. JENSEN*†, JOHN D. MCCALLUM‡, AND JOANN SANDERS-LOEHR‡

Departments of *Biological Structure and †Biochemistry, University of Washington, Seattle, WA 98195; and ‡Department of Chemistry, Portland State University, Portland, OR 97207

Communicated by Harry B. Gray, October 1, 1984

ABSTRACT **The physiologically active forms of the nonheme-iron, oxygen-transport protein hemerythrin have been studied by x-ray crystallographic techniques. At 3.9-Å resolution, a difference electron-density map between the deoxy form and met form (methemerythrin) of the protein suggests only small differences in the binuclear iron complexes. The coordination of the iron atoms appears to be the same in both the deoxy and met forms, one iron of the complexes being pentacoordinate, the other iron being hexacoordinate. The iron atoms appear to be somewhat farther apart in the deoxy form. A 2.2-Å resolution study of oxyhemerythrin shows that dioxygen binds to one iron atom—the pentacoordinate one in the met form of the protein, the same binding site found for azide in azidomethemerythrin.**

The initial objective of the crystallographic structure determinations of hemerythrin was to structurally characterize this nonheme-iron, oxygen-transport protein to provide a basis for understanding the chemical differences between its derivatives. The early studies focused on the structure of the oxidized form, or methemerythrins (1, 2), primarily because they are more stable than are the physiologically more interesting deoxy and oxy forms. The active center is a binuclear iron complex bound to the protein by amino acid side chains. In azidomethemerythrin, the iron atoms are both hexacoordinate (Fig. 1 *Left*). In the met form [formerly identified as aquomet (3) or hydroxomet (4)], one of the iron atoms, designated Fe2, is pentacoordinate (Fig. 1 *Right*). The exogenous ligand binding site is vacant in methemerythrin, with a compensating shift towards trigonal bipyramidal coordination for the five ligands of Fe2. The observation of an oxo-bridged binuclear iron structure in both forms of the protein is consistent with the magnetic and spectroscopic evidence for two strongly coupled high-spin Fe(III) atoms in the metal complex in methemerythrins (5, 6).

Our attention has now shifted to structurally characterizing the deoxy and oxy forms of hemerythrin from *Themiste dyscrita*. The small crystals of deoxyhemerythrin currently available have limited the resolution of our study of this form of the protein to 3.9 Å. Even at this resolution, however, the crystallographic results are valuable because of the limited structural information for deoxyhemerythrin currently available from other techniques. Mossbauer spectroscopy indicates that the complex comprises two high-spin Fe(II) atoms (5, 7), and magnetic susceptibility measurements show little antiferromagnetic coupling between the Fe atoms (5, 8). The absence of a distinct visible absorption spectrum for deoxyhemerythrin has hampered spectroscopic investigations of the Fe complex in this form of the protein.

Larger crystals of oxyhemerythrin have been grown that have enabled us to collect diffraction data for this form of the protein to 2.2-Å resolution. Studies by resonance Raman spectroscopy (9, 10), polarized absorption spectroscopy (11), and x-ray absorption spectroscopy (12) indicate that the metal complex in oxyhemerythrin is similar to that in azidomethemerythrin, where the two Fe(III) atoms are bridged by a μ-oxygen atom, and the exogenous ligand binds only to one Fe atom. The x-ray crystallographic results reported here support this description for oxyhemerythrin and, in addition, suggest some rearrangement in the binuclear iron complex upon conversion from deoxy to oxy. The 2.2-Å resolution crystallographic investigations provide important structural information bearing on the functional properties of the protein and limiting the mechanisms to be considered in explaining the biological action of the molecule.

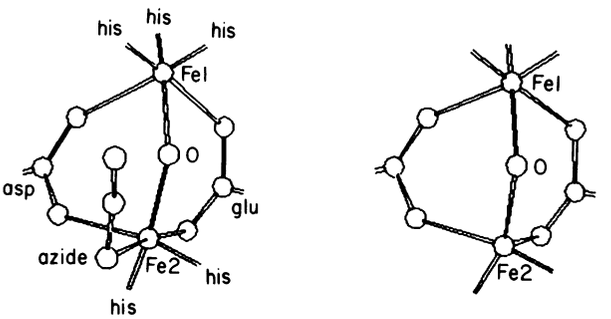

FIG. 1. Structures of the binuclear iron complexes (1) in azidomethemerythrin (*Left*) and methemerythrin (*Right*). The Fe atoms are bound to three histidine side chains, an aspartic acid, a glutamic acid, and a μ-oxo bridging atom derived from the solvent.

EXPERIMENTAL

The sipunculid *T. dyscrita* was obtained from the Oregon Institute of Marine Biology (Charleston, OR). Hemerythrin was extracted and crystallized from the coelomic fluid as described (13, 14). The crystals were dissolved in 0.2 M Tris sulfate (pH 8.0) and concentrated to ≈30 mg of protein per ml by ultrafiltration (XM-50 filter; Amicon). The hemerythrin solution was depleted of oxygen by anaerobic dialysis against nitrogen-purged buffer. A 4-fold molar excess (per hemerythrin monomer) of solid sodium dithionite was added to the dialysis buffer. After 25 hr the protein solution displayed the pale yellow color characteristic of reduced hemerythrin. Crystals of deoxyhemerythrin were obtained by slow dialysis of the concentrated solution against 0.02 M Tris sulfate (pH 7.2) under anaerobic conditions.

Crystals were maintained in the deoxy state by carrying out all crystal-mounting operations in an argon-flushed glove box. Attempts to retain the deoxyhemerythrin crystals failed until the silicone oils and grease used to seal the capillaries were thoroughly degassed. The crystals remained essentially colorless for the duration of data collection, the pink color of oxyhemerythrin being a relatively sensitive internal monitor for the presence for dioxygen.

The publication costs of this article were defrayed in part by page charge payment. This article must therefore be hereby marked "*advertisement*" in accordance with 18 U.S.C. §1734 solely to indicate this fact.

Crystals of deoxyhemerythrin grown by the method described above were much smaller than those used in earlier studies of methemerythrin (3, 15). Their size, about 1/80th of the volume of the methemerythrin crystals, limited the resolution we could achieve. Data were collected on a Picker FACS-1 diffractometer from two crystals, providing a complete data set to 3.9-Å resolution. Both reflections of each Friedel pair were measured by the step-scan technique (16). Empirical absorption (17) and deterioration corrections (18) were applied, and the Friedel mates were averaged to eliminate the effects of anomalous scattering as described elsewhere (18, 19). The data set comprised 5686 reflections of which 4184 were observed with $I > 2\sigma(I)$.

Crystals of oxyhemerythrin suitable for x-ray diffraction were obtained during the initial crystallization of protein from laked blood (14). These crystals were somewhat smaller than the methemerythrin and azidomethemerythrin crystals used in previous studies but were much larger than the deoxyhemerythrin crystals described above. Data to 2.2-Å resolution were collected from six oxyhemerythrin crystals as described for deoxyhemerythrin. The data set comprised 30,587 unique reflections of which 24,608 were observed with $I > 2\sigma(I)$. The crystals remained light pink in color throughout the data collection, but a slight change in color was observed, possibly indicating partial conversion of the protein to methemerythrin.

CALCULATIONS

Difference electron-density maps were calculated for both the oxy and deoxy forms of hemerythrin, comparing them against the met form. The difference coefficients were of the form $|F_0$ (derivative)| − $|F_0$ (methemerythrin)|, and the phases were those calculated for the refined model of methemerythrin (19). The deoxy and oxy structure factors were scaled to those of methemerythrin by equating $\Sigma|F_0$ (derivative)| to $\Sigma|F_0$ (methemerythrin)| for data from 5.0-Å to 3.9-Å resolution for the deoxy derivative and from 5.0-Å to 2.2-Å resolution for the oxy derivative. The index R' [$=\Sigma||F_0$ (derivative)| − $|F_0$ (methemerythrin)$||/\Sigma|F_0$ (derivative)|] was 0.124 for the deoxy and 0.086 for the oxy derivatives.

For purposes of comparison and calibration, we also calculated the difference electron density, comparing the azidomet form against the met form of the protein at both 3.9-Å and 2.2-Å resolution. In previous comparisons of these forms, we found the major changes caused by binding of the exogenous ligand to be located near Fe2. Accordingly, we calculated the difference electron density in the plane defined by Fe2—the μ-oxo bridge and the azide nitrogen atom bound to Fe2 in azidomethemerythrin. Difference electron densities were calculated for each of the four subunits in the asymmetric unit and subsequently were averaged to increase the signal-to-noise ratio. Fig. 2 shows the averaged difference electron densities for azidomet − met forms and deoxy − met forms, both at 3.9-Å resolution, while Fig. 3 shows difference electron densities for azidomet − met and oxy − met forms, both at 2.2-Å resolution.

RESULTS AND DISCUSSION

The sections shown in Figs. 2*a* and 3*a* from the 3.9-Å and 2.2-Å azidomet − met difference electron density maps are included for comparative purposes. At 3.9-Å resolution (Fig. 2*a*), the bound azide is indicated by a prominent region of positive density shifted somewhat towards the bridging μ-oxygen atom. The region of negative density to the left of Fe2 and the gradient in the density at Fe2 indicate a shift of that atom towards the azide ligand, a shift consistent with the change from pentacoordinate iron in methemerythrin to hexacoordinated iron in azidomethemerythrin.

Although the major differences between the azidomet and

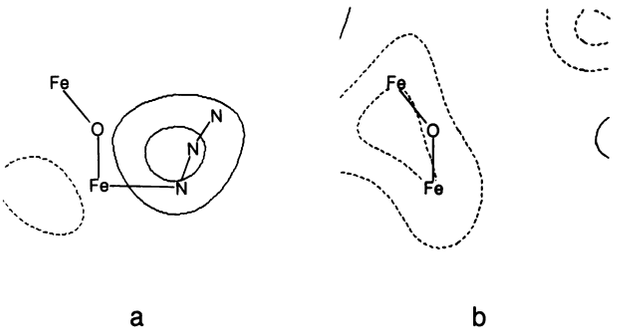

FIG. 2. Difference electron density maps in the plane $O_{\mu\text{-oxo}}$—Fe2—N_{azide}. (*a*) Azidomet − met forms at 3.9-Å resolution. Atom positions are from the 2.0-Å resolution refinement of azidomethemerythrin. Contours are at intervals of 0.315 $e^-/Å^3$, with the zero contour omitted. (*b*) Deoxy − met forms at 3.9-Å resolution. Contours are at intervals of 0.06 $e^-/Å^3$, with the zero contour omitted. —, Positive electron density; ---, negative electron density.

met structures are evident at 3.9-Å resolution, the difference density at 2.2-Å resolution shown in Fig. 3*a* is much more definitive. The electron density of the bound azide is much greater at higher resolution and, in addition, is elongated along the axis of the ligand and essentially centered on it. The shift of Fe2 suggested in Fig. 2*a* is now clearly shown by the steep gradient in the density at that atom in Fig. 3*a*. Comparison of Figs. 2*a* and 3*a* indicates that the positive shift density, the peak to the right of Fe2 in Fig. 3 that is resolved at 2.2-Å resolution, merges with the azide peak at lower resolution and shifts the center of the electron density.

The difference electron densities for deoxy − met and oxy − met forms shown in Figs. 2*b* and 3*b*, respectively, are contoured at levels one-fifth those for the azidomet − met sections in Figs. 2*a* and 3*a*. Thus, the densities in Figs. 2*b* and 3*b* are much less in absolute terms than those in Figs. 2*a* and 3*a*. In the case of the deoxy − met map, the lower density suggests smaller structural differences than does the azidomet − met map, while in the oxy − met map, the lower density is more likely due to loss of oxygen—i.e., to partial conversion to methemerythrin. It is unlikely that any residual deoxyhemerythrin would remain, in view of the high oxygen affinity of the deoxy form. Facilities are not yet available for us to spectroscopically determine occupancies in single crystals. Accordingly, we have compared the azidomet − met and oxy − met electron densities (Fig. 3 *a* and *b*) to obtain an estimate of the occupancy of the oxyhemerythrin crystals. On the basis of peak heights and the number of electrons in

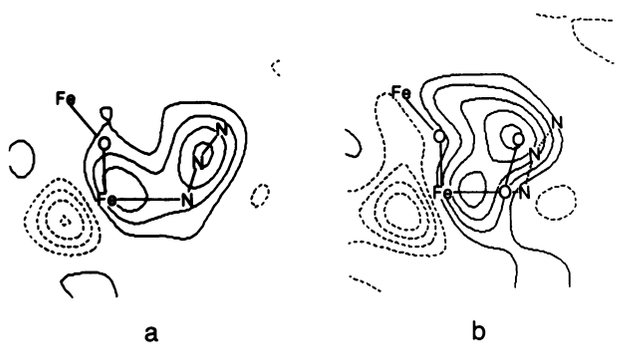

FIG. 3. Difference electron density maps in the plane $O_{\mu\text{-oxo}}$—Fe2—N_{azide}. (*a*) Azidomet − met forms at 2.2-Å resolution. Contours are at intervals of 0.315 $e^-/Å^3$, with the zero contour omitted. (*b*) Oxy − met forms at 2.2-Å resolution. Azidomet atoms were as in Fig. 2*a*; dioxygen atom locations were estimated from the present map. Contours are at intervals of 0.06 $e^-/Å^3$, with the zero contour omitted. —, Positive electron density; ---, negative electron density.

azide and dioxygen, we estimate the occupancy of the dioxygen site to be no less than one-third.

Although results at low resolution must be regarded as tentative, the complex in the deoxy form appears to retain the same ligands and symmetry as the complex in the met form. Comparison of Fig. 2 *a* and *b* emphasizes the absence of any density in the deoxy form at the exogenous ligand site, and there is no indication of the lateral shift of Fe2 found when small molecules bind to the met form. The only difference appears to be a gradient in the density at the iron sites in Fig. 2*b*, suggesting that these atoms are farther apart in the deoxy form than in the met form. The increase in the Fe–Fe distance in the deoxy form is consistent with the extended x-ray absorption fine structure (EXAFS) results, indicating that the correlated motion of the Fe atoms has decreased in that form (20) and the short Fe—$O_{\mu\text{-oxo}}$ bonds are no longer evident (20). Although the unusual temperature dependence of the EXAFS is best explained by a breakage of one of the bridging Fe—$O_{\mu\text{-oxo}}$ bonds (20), the difference electron density in Fig. 2*b* shows no indication of this.

The difference electron density in the oxy − met map (Fig. 3*b*) exhibits a broad peak in the region of the exogenous ligand site, the peak extending almost to the Fe1—$O_{\mu\text{-oxo}}$ bond, and a relatively steep gradient in the density at Fe2, similar to that observed in the azidomet − met map (Fig. 3*a*). The gradient at Fe2 is definitive evidence for the shift in position of that atom caused by the bound dioxygen (1). In addition, a gradient in density at both Fe1 and the μ-oxo bridging atom is also evident in Fig. 3*b*, indicating shifts in the positions of both atoms. The positive shift densities associated with these atoms will account in part for the breadth of the peak representing the bound dioxygen. It should be observed, however, that the peak is shifted somewhat towards the Fe–Fe axis of the complex, compared to the azide peak in Fig. 3*a*. A model consistent with the observed density has the dioxygen bound to Fe2 with both oxygen atoms shifted somewhat towards the Fe–Fe axis relative to the azide ligand in azidomethemerythrin.

Resonance Raman experiments have characterized the bound dioxygen as a peroxo species (9). A question then arises concerning the stabilization of the bound O_2. A charged species such as peroxide would be expected to bind either side-on as in (OEP)Ti(O_2) (ref. 21; where OEP = octaethylporphyrin) or end-on and protonated as in $[(en)_2Co(O_2H)(NH_2)Co(en)_2]^{4+}$ (ref. 22; where en = ethylenediamine). The difference electron density for the oxy − met forms essentially rules out side-on binding of the dioxygen. Thus, it is likely that the peroxo species is protonated. In addition, it may be involved in hydrogen bonding to stabilize its binding to the complex. In oxyhemoglobin, the dioxygen described as a superoxo anion (23) is hydrogen-bonded to the distal histidine (24, 25), the overall oxygen environment being hydrophobic in nature. In oxyhemerythrin, the O_2 binding site is also quite hydrophobic, and the only protein side chains in the vicinity of the bound dioxygen are aliphatic side chains whose interactions with O_2 appear to be van der Waals contacts. The only hydrogen bond acceptor near the dioxygen is the oxygen atom in the μ-oxo bridge. A hydrogen bond in this location could contribute to the differences in dioxygen and azide binding observed. A similar proposal has been made to account for deuterium isotope effects and the Fe—O—Fe vibration frequencies in the resonance Raman spectrum of oxyhemerythrin (10).

Although a hydrogen bond would stabilize the peroxo anion, a question arises concerning the mechanics of providing a proton for the hydrogen bond. An attractive hypothesis, yet to be confirmed or refuted by experiment, invokes hydroxyl as the bridging group in deoxyhemerythrin and holds that when dioxygen binds, the proton shifts onto the peroxo anion, leaving a μ-oxo bridge between the Fe atoms. This is shown schematically in Fig. 4. The lack of any pH dependency in the conversion between deoxy and oxyhemerythrin is consistent with this hypothesis (26). This mechanism also would explain the longer Fe–Fe distance in deoxyhemerythrin since Fe—OH_μ bonds are expected to be longer than Fe—$O_{\mu\text{-oxo}}$ bonds. It should be noted that in one model complex protonation of the bridging oxygen with no change in the oxidation state does lengthen the Fe—O distances (27).

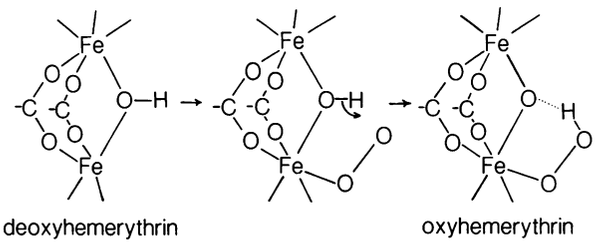

FIG. 4. Proposed mechanism of conversion of deoxyhemerythrin to oxyhemerythrin.

Another structural feature of the protein bearing on the oxygenation process concerns the access pathway of dioxygen to the metal center. Although the dynamical nature of proteins does not require open channels in macromolecules for diffusion of small ligands or substrates, it is still useful to search for regions of the protein structure that might be more likely candidates for functional crevices or pathways. Soon after the hemerythrin structure was solved, we suggested a route to the metal center by way of an extended channel between and parallel to the α helices, a distance of 15–20 Å (28). However, another structural feature observed in a molecular model of hemerythrin suggests another possible route. The region between helices C and D is filled with four interleaving, parallel aromatic side chains (29). A gap between the side chains of His-101 and Trp-97 leads directly to the ligand binding site at the complex. The distance from the complex to the surface of the protein by way of this gap is 10 Å, suggesting that this is a much more likely route for ligands to approach the complex.

SUMMARY

The models that best account for the difference electron densities for deoxy and oxyhemerythrin are presented in Fig. 4. The active site in deoxyhemerythrin appears rather similar to that in methemerythrin but with the Fe atoms separated by a somewhat greater distance. The binuclear complex in oxyhemerythrin is similar to that found in other oxidized forms of the protein such as azidomethemerythrin, but with the dioxygen located slightly closer to the μ-oxygen atom. The oxyhemerythrin structure with end-on binding of hydroperoxide to a μ-oxo bridged binuclear iron center was originally proposed by Gray (30) and has since been supported by a number of different spectroscopic investigations (9–12). Although there is good agreement between the present crystallographic results and the spectroscopic and magnetic data on oxyhemerythrin and deoxyhemerythrin, higher resolution studies are needed to provide more definitive structural information on these biologically active complexes.

We thank K. D. Watenpaugh for the program used to calculate the arbitrarily oriented sections of the electron density maps. This work has been supported by grants GM-10828 (L.H.J.) and GM-18865 (J.S.-L.) from the National Institutes of Health and an equipment grant (PCM 76-20557) from the National Science Foundation.

1. Stenkamp, R. E., Sieker, L. C. & Jensen, L. H. (1984) *J. Am. Chem. Soc.* **106**, 618–622.

2. Hendrickson, W. A. (1981) in *Invertebrate Oxygen-Binding Proteins: Structure, Active Site and Function*, eds. Lamy, J. & Lamy, J. (Dekker, New York), p. 503.
3. Stenkamp, R. E., Sieker, L. C. & Jensen, L. H. (1983) *J. Inorg. Biochem.* **19,** 247–253.
4. Stenkamp, R. E., Sieker, L. C. & Jensen, L. H. (1982) *Acta Crystallogr. Sect. B* **38,** 784–792.
5. Garbett, K., Darnall, D. W., Klotz, I. M. & Williams, R. J. P. (1969) *Arch. Biochem. Biophys.* **135,** 419–434.
6. Dawson, J. W., Gray, H. B., Hoenig, H. E., Rossman, G. R., Schredder, J. M. & Wang, R. H. (1972) *Biochemistry* **11,** 461–465.
7. York, J. L. & Bearden, A. J. (1970) *Biochemistry* **9,** 4549–4554.
8. Okamura, M. Y., Klotz, I. M., Johnson, C. E., Winter, M. R. C. & Williams, R. J. P. (1969) *Biochemistry* **8,** 1951–1958.
9. Kurtz, D. M., Shriver, D. F. & Klotz, I. M. (1977) *Coord. Chem. Rev.* **24,** 145–178.
10. Shiemke, A. K., Loehr, T. M. & Sanders-Loehr, J. (1984) *J. Am. Chem. Soc.* **106,** 4951–4956.
11. Gay, R. R. & Solomon, E. I. (1978) *J. Am. Chem. Soc.* **100,** 1972–1973.
12. Elam, W. T., Stern, E. A., McCallum, J. D. & Sanders-Loehr, J. (1982) *J. Am. Chem. Soc.* **104,** 6369–6373.
13. Klotz, I. M., Klotz, T. A. & Fiess, H. A. (1957) *Arch. Biochem. Biophys.* **68,** 284–299.
14. Dunn, J. B. R., Addison, A. W., Bruce, R. E., Loehr, J. S. & Loehr, T. M. (1977) *Biochemistry* **16,** 1743–1749.
15. Stenkamp, R. E., Sieker, L. C., Jensen, L. H. & Sanders-Loehr, J. S. (1981) *Nature (London)* **291,** 263–264.
16. Hanson, J. C., Watenpaugh, K. D., Sieker, L. C. & Jensen, L. H. (1979) *Acta Crystallogr. Sect. A* **35,** 616–621.
17. North, A. C. T., Phillips, D. C. & Mathews, F. S. (1968) *Acta Crystallogr. Sect. A* **24,** 351–359.
18. Stenkamp, R. E., Sieker, L. C. & Jensen, L. H. (1982) *Acta Crystallogr. Sect. B* **38,** 784–792.
19. Stenkamp, R. E., Sieker, L. C. & Jensen, L. H. (1983) *Acta Crystallogr. Sect. B* **39,** 697–703.
20. Elam, W. T., Stern, E. A., McCallum, J. D. & Sanders-Loehr, J. (1982) *J. Am. Chem. Soc.* **105,** 1919–1923.
21. Guilard, R., Latour, J.-M., Lecomte, C., Marchon, J.-C., Protas, J. & Ripoll, D. (1978) *Inorg. Chem.* **17,** 1228–1237.
22. Thewalt, U. & Marsh, R. (1967) *J. Am. Chem. Soc.* **89,** 6364–6365.
23. Barlow, C. H., Maxwell, J. C., Wallace, W. J. & Caughey, W. S. (1973) *Biochem. Biophys. Res. Commun.* **55,** 91–95.
24. Kitagawa, T., Ondrias, M. R., Rousseau, D. L., Ikeda-Saito, M. & Yonetani, T. (1982) *Nature (London)* **293,** 869–871.
25. Phillips, S. E. V. & Schoenborn, B. P. (1981) *Nature (London)* **292,** 81–82.
26. de Waal, D. J. A. & Wilkins, R. G. (1976) *J. Biol. Chem.* **251,** 2339–2343.
27. Armstrong, W. H. & Lippard, S. J. (1984) *J. Am. Chem. Soc.* **106,** 4632–4633.
28. Stenkamp, R. E., Sieker, L. C. & Jensen, L. H. (1978) *J. Mol. Biol.* **126,** 457–466.
29. Sieker, L. C., Stenkamp, R. E. & Jensen, L. H. (1982) in *The Biological Chemistry of Iron*, eds. Dunford, B., Dolphin, D., Raymond, K. & Sieker, L. (Reidel, Dordrecht, Netherlands), pp. 161–175.
30. Gray, H. B. (1971) *Adv. Chem. Ser.* **100,** 365–389.